

REPORT DOCUMENTATION PAGE

AFRL-SR-AR-TR-04-

Public reporting burden for this collection of information is estimated to average 1 hour per response, including the time for reviewing instructions, gathering existing data needed, and completing and reviewing this collection of information. Send comments regarding this burden estimate or any other aspect of this burden to Department of Defense, Washington Headquarters Services, Directorate for Information Operations and Reports (0704-018) 4302. Respondents should be aware that notwithstanding any other provision of law, no person shall be subject to any penalty for failing to provide information if it does not have a valid OMB control number. PLEASE DO NOT RETURN YOUR FORM TO THE ABOVE ADDRESS.

0107

1. REPORT DATE (DD-MM-YYYY) 02-16-2004		2. REPORT TYPE Final		3. DATES COVERED (From - To) 01/01/01 - 12/31/03	
4. TITLE AND SUBTITLE Optimizing Mechanical Properties & Thermal Stability of Age Hardenable Aluminum Alloys through Theoretical Modeling, Alloy Modification & Thermal Mechanical Properties				5a. CONTRACT NUMBER N/A	
				5b. GRANT NUMBER F49620-01-1-0090	
				5c. PROGRAM ELEMENT NUMBER N/A	
6. AUTHOR(S) Starke, E. A.				5d. PROJECT NUMBER N/A	
				5e. TASK NUMBER N/A	
				5f. WORK UNIT NUMBER N/A	
7. PERFORMING ORGANIZATION NAME(S) AND ADDRESS(ES) University of Virginia Office of Sponsored Programs P. O. Box 400195 Charlottesville, Virginia 22904-4195				8. PERFORMING ORGANIZATION REPORT NUMBER 110765-101-GG10112-31340 (FAS #5-25896)	
9. SPONSORING / MONITORING AGENCY NAME(S) AND ADDRESS(ES) Air Office of Scientific Research 4015 Wilson Blvd., Rm. 713 Arlington, Virginia 22203-1954				10. SPONSOR/MONITOR'S ACRONYM(S) N/A	
				11. SPONSOR/MONITOR'S REPORT NUMBER(S) N/A	
12. DISTRIBUTION / AVAILABILITY STATEMENT Approved for public release, distribution unlimited.					
13. SUPPLEMENTARY NOTES N/A					
14. ABSTRACT This research was concerned with a practical approach to the design of an improved age-hardenable aluminum alloy for moderate temperature application. The process involved extensive empirical research, theoretical simulation and modeling, calculated phase diagrams and first principle calculations & analytical techniques. Microstructure characterization and analytical transmission electron microscopy were employed to refine the development of the quaternary Al-Cu-Mg-Ag phase diagram. Differential scanning calorimetry & electron diffraction were implemented to investigate the microstructural evolution of the ternary alloys & to validate calculated equilibrium phase boundaries. Energy dispersive spectroscopy was also used to illustrate the effect of trace additions on the phase boundaries that are important for the thermal stability of this class of alloys. Computer simulation & modeling were used to identify the microstructure that will result in the optimal combination of mechanical properties. Unavailable parameters were calculated from first principle atomistic modeling. The major objective of this research program has been to illustrate the use of modeling & simulation in alloy design & therefore aid in the early insertion of new high performance materials.					
15. SUBJECT TERMS age-hardenable aluminum alloy, microstructure characterization, analytical transmission electron microscopy					
16. SECURITY CLASSIFICATION OF:			17. LIMITATION OF ABSTRACT UL	18. NUMBER OF PAGES 16	19a. NAME OF RESPONSIBLE PERSON Starke, E. A.
a. REPORT Unclassified	b. ABSTRACT Unclassified	c. THIS PAGE Unclassified			19b. TELEPHONE NUMBER (include area code) 434-924-6332

20040225 155

Final Report

OPTIMIZING MECHANICAL PROPERTIES AND THERMAL STABILITY OF AGE HARDENABLE ALUMINUM ALLOYS THROUGH THEORETICAL MODELING, ALLOY MODIFICATION AND THERMAL MECHANICAL PROCESSING AFOSR GRANT S49620-01-1-0090

Aiwu Zhu, B.M. Gable, G.J. Shiflet and Edgar A. Starke, Jr.
Department of Materials Science and Engineering
University of Virginia
116 Engineer's Way
P.O. Box 400745
Charlottesville, VA 22904-4745

ABSTRACT

This research was concerned with a practical approach to the design of an improved age-hardenable aluminum alloy for moderate temperature application. The process involved extensive empirical research, theoretical simulation and modeling, calculated phase diagrams and first principle calculations and analytical techniques. Microstructure characterization and analytical transmission electron microscopy were employed to refine the development of the quaternary Al-Cu-Mg-Ag phase diagram. Differential scanning calorimetry and electron diffraction were implemented to investigate the microstructural evolution of the ternary alloys and to validate calculated equilibrium phase boundaries. Energy dispersive spectroscopy was also used to illustrate the effect of trace additions on the phase boundaries that are important for the thermal stability of this class of alloys. Computer simulation and modeling were used to identify the microstructure that will result in the optimal combination of mechanical properties. Unavailable parameters were calculated from first principle atomistic modeling. The major objective of this research program has been to illustrate the use of modeling and simulation in alloy design and therefore aid in the early insertion of new high performance materials.

INTRODUCTION AND TECHNICAL BACKGROUND

Due to economic considerations, alloy design and development can no longer be performed using the purely empirical, trial and error approach that has been dominate over the past 100 years. Modeling and simulation, in conjunction with experiments, can be employed to improve the efficiency of alloy design, optimizing processing and manufacturing operations. This approach can greatly reduce the time associated with alloy development and the generation of the knowledge base required for insertion of new materials into aerospace systems. This research and development program was aimed at obtaining a high-strength, thermally stable aluminum-based alloy that would be suitable for moderate temperature applications up to approximately 150°C, that could be used for the fuselage of a Mach 2.2-2.4 aircraft. Ultimately, the objective of this research is to provide an example of streamlined alloy design based upon the marriage of theoretical metallurgical principles, calculated phase diagrams and experimental alloy design and processing. An outline of the approach undertaken for this program is schematically represented in Figure 1.

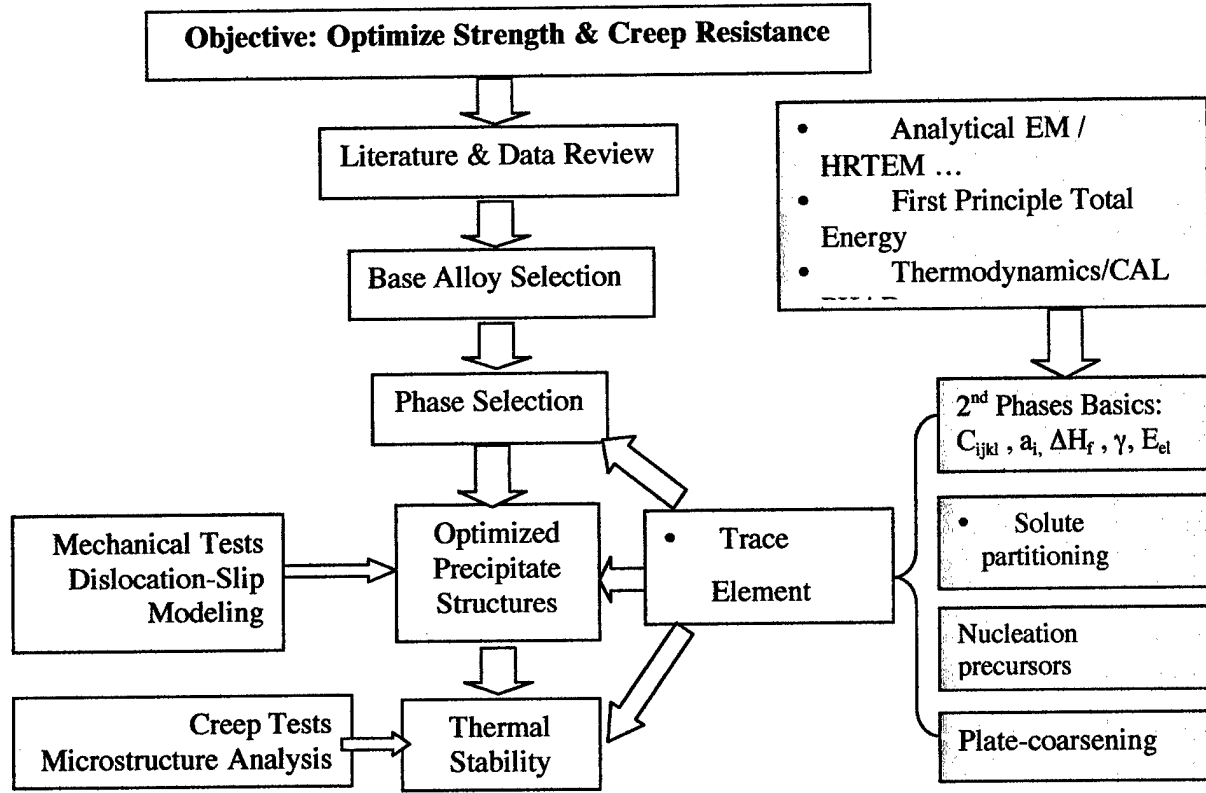


Figure 1 – Alloy development methodology

The first step in alloy design is to select a system that offers promise for obtaining the desired microstructure and properties. After an extensive literature search and examination of empirical data, we selected the Al-Cu-Mg-(Ag) system for our base system. In order to identify the optimized precipitate structure and morphology, our research team developed a dislocation-slip simulation method [1]. In combination with a quantitative microstructure characterization procedure, we have been able to evaluate superposition of the strengthening effects of precipitates with different volume fractions, sizes, shapes (aspect ratio) and orientations with respect to the Al-matrix. This has allowed us to find the optimized precipitate-structure for maximum strength. For instance in an Al-Li-Cu alloy where the main strengthening precipitates are T_1 -{111} and θ' -{100} plates, a structure comparison factor κ_{AB} can be introduced to describe the superposition effects,

$$\kappa_{AB} = \zeta \left(\frac{D_A}{D_B} \right)^2 / \left(\frac{\gamma_A}{\gamma_B} \cdot \frac{V_{m,A}}{V_{m,B}} \cdot \frac{\sin \theta_A}{\sin \theta_B} \right) \quad (1)$$

where the coefficient ζ accounts for the effect of plate orientation, D_A and γ_A are the mean diameter and the aspect ratio of the A-plates, respectively, and D_B and γ_B for those of the B-plates. We have shown that co-existence of both T_1 {111} and θ' {100} plates in certain combinations has the highest overall strengthening effect for a given Cu-composition [1]. The knowledge gained through the simulation has been verified in some Al-alloys [1,2]. Regarding the Al-Cu-Mg-Ag-X system, have been concerned with Ω (Al_2Cu), a plate-like phase with a

$\{111\}_\alpha$ habit plane, $\theta'(\text{Al}_2\text{Cu})$ plate-like phase with a $\{100\}_\alpha$ habit-plane, and S (Al_2CuMg) a rod-like phase oriented along the $\langle 210 \rangle_\alpha$ direction. These three phases may co-exist in many Al-Cu-Mg-Ag alloys under conventional processing conditions. The rod-like S or S' phase is less effective in the strengthening, possibly due to its particular orientation, which results in relatively small obstacles to dislocation motion on $\{111\}_\alpha$ slip planes. Our dislocation-slip simulations have shown that for optimal strength, the coexistence of a fine uniform distribution of θ' and Ω plates in certain combinations is desired.

The Al-Cu-Mg-(Ag) System: We selected this system after an examination of the literature and available empirical data. The strengthening precipitates, especially the $\{100\}_\alpha$ Al_2Cu phase (θ'/θ), in the Al-Cu-Mg-X 2xxx alloy system are more thermally stable at moderate temperatures than those present in the Al-Zn-Mg-X 7xxx or the Al-Si-Mg 6xxx alloy systems. The addition of small amounts of Ag, on the order of 0.4 wt%, to Al-Cu-Mg-X alloys with high Cu:Mg ratios (e.g. 10:1 wt%) has been shown to significantly enhance the age hardening response over that of a similar ternary alloy (c.f. [3]). The marked gain in strength is due to the formation of a uniform dispersion of a hexagonal plate precipitate with a $\{111\}_\alpha$ habit plane, designated Ω . Several detailed studies have indicated that the internal crystal structure of the Ω plates is quite similar to that of equilibrium θ ([4-8]). As will be described later, we have assessed the validity of this assumption.

It has recently been shown that Ag facilitates Ag-Mg clusters that in turn act as nucleation sites for the Ω phase [9,10]. Detailed atom probe and high resolution Z-contrast microscopy have revealed that Ag and Mg are present at the coherent interfaces between the Ω plate and the enveloping aluminum matrix [9-11]. Two prominent factors that jeopardize the fine uniform distribution of Ω plates in the quaternary alloys have also been identified. The long-term stability of the Ω plate is sensitive to the presence of S-phase precipitation (Al_2CuMg). If the alloy composition lies within the equilibrium ($\alpha + \theta + \text{S}$) phase field the existence of S-phase will create chemical potential (μ) gradients in Mg. Essentially the presence of S-phase limits the Mg available for the coherent interfaces of the Ω plates. Similarly, several studies have illustrated Ag segregation to S-phase in this class of quaternary alloys [10,12]. The presence of S-phase is deleterious to the stability and coarsening resistance of Ω plates due to the fact that the Ω plates may only exist with Mg and/or Ag at the coherent interfaces. The first goal was to design a quaternary alloy that lies within the ($\alpha + \theta$) phase field for a wide range of desirable temperatures. Therefore, we must have a thorough understanding of phase space for both the Al-Cu-Mg ternary and the Al-Cu-Mg-Ag quaternary Al-rich alloys. Once within the ($\alpha + \theta$) phase field the driving force for coarsening of the Ω plates must be quelled in order to maintain a fine uniform and thermally stable distribution.

Phase Diagram and Thermodynamic Modeling: The CALPHAD method (CALculation of PHase Diagrams) is an approach to establishing equilibria among phases, through thermodynamic modeling of the individual phases based on the idea of phase competition in a system. The phases are modeled according to the phase stabilities, measured thermodynamic properties, and the measured transus points (including liquidus, solidus, eutectic, etc). In our research, differential scanning calorimetry (DSC) is used to establish thermal events associated with phase transformations, X-ray and electron diffraction determine structure and analytical

electron microscopy may all be used to validate equilibrium phase boundaries calculated with the CALPHAD techniques.

For alloy systems, phases may be formally treated using a sub-lattice concept. For ternary non-ideal solutions, their Gibbs energy, using a sub-regular model, may be expressed in a Redlich-Kirst-Muggianu's formula,

$$\phi G = \sum_i^n x_i \phi G_i^0 + RT \sum_{i=1}^n x_i \ln x_i + \sum_{i \neq j}^n x_i x_j \sum_{k=0}^m {}^i L_{i,j}^{(k)} (x_i - x_j^{(k)}) + \sum_{i \neq j \neq l}^n x_i x_j x_l \sum_k \phi L_k V_k \quad (2)$$

The specific models employed and the interaction parameters L between elements, *e.g.*, i and j for each phase, are compiled in a database. Retrieving the data from the database, a software-package Thermo-Calc can then be used to determine the stable phases present in a system as a function of composition, temperature and pressure. The stable phases are determined from the relative minimum in the Gibbs free energy term for each phase possible in the system.

Regarding the Al-Cu-Mg-(Ag)-X (X=Si, Zn, Ce...) system, well-developed databases for Al-Cu-Mg, Al-Cu-Si, Al-Mg-Si, Al-Cu-Mg-Zn etc. are available. The elements including Al, Si, Mg, Zn, Ce *etc.* are considered in a light-alloy database called "COST507" [13] developed by a European group with participants of 14 EU countries. We also have been using the database TT-Al [14] that is useful for solidification studies near the Al-rich corner of the system. Effort was also made for the construction of an Al-Cu-Mg-Ag database [15]. However, the most significant information for our alloy design purpose, particularly in the Al-rich corner, were either missing or incomplete:

- 1) Both Ω and θ' , the selected strengthening phases, have not been modeled;
- 2) The S phase was modeled but Ag-partitioning, the controlling factor for phase competition with Ω and θ' , was not incorporated.
- 3) The effects of the trace element, *e.g.*, Si, Zn, Ce *etc.*, have not been characterized.

The first critical component needed to optimize this class of alloys is to control the bulk composition so that it lies within the (α -FCC + θ' + Ω) phase field in order to avoid S-phase precipitation during aging treatment (since S-particles are less effective in strengthening and act to remove Mg and Ag from the Ω interface which leads to the dissolution of the Ω plates). To optimize the Al-Cu-Mg-Ag quaternary system the (α + θ' + Ω)/(α + θ' + Ω +S) phase boundary must be accurately located and determined as a function of bulk composition, artificial aging time and temperature. The databases can also be used, as shown below, for evaluation of some properties that are reflected in the thermodynamics of the system.

Formation of the Desired Precipitate Structure: In the Al-Cu-Mg-Ag-X system, θ' -precipitates evolve from clustering of Cu on $\{100\}_\alpha$ -planes in Al-FCC. The nucleation of Ω -plates is assisted by clustering or short-range ordering of Cu-Mg and/or Ag-Mg, that act as precursors, as observed in [9,10]. Since the formation of the undesired S-phase will consume Cu, Mg and Ag from the matrix, this phase is deleterious for the nucleation of the θ' - and particularly Ω -phase and, hence, for the formation of the desired (θ' + Ω) structure. Dislocations introduced by pre-age plastic transformation, the T8-treatment, were also found to favor the nucleation of θ' [16]. The strategy for our plan for increasing the nucleation rate of the Ω phase

focused on the enhancement of the formation of precursors (clusters or SROs) by trace additions. The desired ($\theta' + \Omega$) structure with a fine and uniform distribution will eventually be produced through rigid control of Cu and Mg contents, trace element additions and using refined thermo-mechanical processing.

Thermal Stability of the Desired Precipitate Structures: The coarsening behavior of the Ω plates in Al-Cu-Mg-Ag has been extensively studied in our lab [11]. The coarsening or thickening rate is slower when the thickness of Ω -plates is less than $\sim 13\text{nm}$. This may be attributed to the inability to form the misfit compensating *in-situ* dislocations at the edge interface between the plates and the matrix. The vacancy (dilation) strain associated with the (-9%) misfit between the single Ω unit cell high Ω -plates and $2\{111\}_\alpha$ plane spacing makes the nucleation of thickening ledges difficult, particularly during the coarsening stage where the driving forces will be much lower than during growth. When the plates are thicker than the critical value, acceleration in thickening occurs due to the relaxation of the strain field with the formation of the misfit dislocations. Another important finding is the trace element segregation in the broad interfaces of Ω plates.

More generally, there are two issues for the thermal stability of a precipitate structure containing more than one 2nd phase – phase coarsening and phase competition from other phases. Coarsening of a single 2nd phase is thermodynamically attributed to the tendency for decreasing the total interfacial energy between the 2nd phase and the Al-matrix. The interfacial energy may consist of the chemical energy, as described by the bond-breaking model, and the associated strain energy. Trace element additions may have two possibly “useful” ways of partitioning: either segregating at the interfaces or being soluble in the 2nd phase. The former alters the chemistry of the interfaces, e.g. Ag layers observed by Z-contrast HRTEM [11], possibly leading to a lower interfacial energy. The partitioning into the 2nd phase, like the Zn-partitioning in T_1 phase [17], changes the lattice constants and may hence modify the misfit strain. It was also shown that Ag segregates to S phase in an Al-Cu-Mg-Ag alloy [10]. On the other hand, different from the simple alloys in the two-phase field, the coarsening behavior of higher-order alloys like the Al-Mg-Cu-(Ag)-(Si)-X system containing more than one 2nd phase (like Ω , θ' and S) is also affected by the competition from other 2nd phases for the solute Cu, Mg and/or Ag that they share. For example at service temperatures ($<150^\circ\text{C}$) usually lower than aging-treatment temperatures $>200^\circ\text{C}$, the driving force for formation of S-phase will inevitably become significant. The formation of S-phase consuming the solute Mg and Ag, that are stabilizers for Ω , and Cu in the Al matrix and, hence, make both θ' and Ω particles less stable leading to potential dissolution. Therefore, our objective here is not only to lower the coarsening rate of the Ω and θ' -plates but also to prevent the S-phase from jeopardizing the stability of the Ω plates.

First Principle Calculations: Crystal Structure, Elastic Constants and Interfacial Energies: Although the precipitate phases (Ω , θ' , S, etc.) in this system have been known for years, some fundamental properties such as crystal structure, enthalpy of formation, deformation behavior and interfacial energy between these phases and the Al matrix are not available because of difficulties in experimental measurement. These data are necessary for any reliable quantitative thermodynamic and kinetic analysis of this system.

First principle total energy calculations are being employed for this purpose. We have been using the Vienna ab initio simulation program (VASP) [18] where the density functional theory plane-wave pseudo-potential method is applied. Mainly LDA (Local-Density Approximation) is used for electronic exchange correlation potentials. GGA (general gradient approximation), such as PWE and PW91 functionals, are also being tested. The ultrasoft pseudo-potentials, supplied with the VASP-package, are utilized. The GGA did not produce any significant changes in most of our results. The basis-set cut-offs were set to "high accuracy" and k-point meshes are set by "Monkhorst-Pack" (or Γ -centered) setting from $8 \times 8 \times 8$ to $32 \times 32 \times 32$ (or otherwise indicated) depending on the size of the unit cell concerned.

Crystal Structures and Formation Enthalpy: The first principle energy calculations are used to validate the proposed crystal structures and to calculate the formation energies of various precipitates. It offers some important data that are unavailable from an empirical approach. The formation enthalpies obtained may be used for input in the CALPHAD database development. For a binary phase A_pB_q , the formation enthalpy is defined as the energy gain or loss with respect to the bulk constituents A and B at their equilibrium lattice constants

$$\Delta H^{eq}(A_pB_q) = E^{eq}(A_pB_q) - x_A E^{eq}(A) - x_B E^{eq}(B) \quad (3)$$

where $E^{eq}(A_pB_q)$ and $E^{eq}(A)$ and $E^{eq}(B)$ are the energies of the second phase A_pB_q and the constituents A and B. $x_A = p/(p+q)$ and $x_B = q/(p+q)$ are the concentrations of A and B. The formation energy corresponds to geometrically fully relaxed compounds, i.e., the structures are optimized (consistent with the symmetry of the structure) with respect to unit cell vectors, atomic displacements and volume of the unit cell.

θ' and θ -phases: The tetragonal crystal structures, including space group, internal atomic coordinates and lattice constants of θ' and θ -phases have been known for some time. Our calculations gave the formation enthalpies and validated the lattice constants as shown in Table I.

Table I. Experimental and Calculated Lattice Constants and Calculated Enthalpy of θ' and θ -phases

Phase	Lattice Constants- Experimental, Å	Lattice Constants- Calculated, Å	Enthalpy of Formation- Calculated, eV/atom
θ'	A= 4.04, c= 5.80	4.0756, 4.0756, 5.8294	-0.213
θ	A=6.063, c=4.87	6.074, 6.074, 4.850	-0.168

Ω Phase: Several crystal structures for the Ω phase have been proposed. Auld suggested a monoclinic structure [4]. A widely accepted structure [7] is orthorhombic with space group (Fmmm). Based on analysis of the convergent-beam electron diffraction (CBED) patterns, Garg and Howe [8] advocated a tetragonal structure (I4/mcm) that is only a metastable $\{111\}_\alpha$ variant of the equilibrium θ phase. Table II lists our calculated results using VASP. It shows that the proposed monoclinic structure has a positive formation enthalpy and hence is unreasonable. Both

the tetragonal and the orthorhombic structures have formation enthalpies that are close to that of the equilibrium θ phase. According to the COST 507 database that was compiled via the CALPHAD method, the formation enthalpy of the equilibrium θ phase is -161 meV/atom. Experiments have yielded values from -245 to -135 meV/atom [19]. Due to the similarity of the calculated formation enthalpy of Ω to that of equilibrium θ , Ω may be regarded as a metastable $\{111\}_\alpha$ variant of θ .

Table II. VASP Calculated Formation Enthalpies and the Vector Lengths (unit cell) of Proposed Crystal Structures for the Ω phase.

	Proposed	H, eV/atom	Vector Length, Å
Equilibrium θ	Tetragonal (I4/mcm): 6.063, 4.87	-0.168	6.074, 6.074, 4.850
Auld's	Monoclinic: a = b:4.96, c:8.48, 120	0.195	4.930, 4.930, 9.122
Knowles'	Orthorhombic (Fmmm):4.96, 8.59, 8.46	-0.167	4.8946, 8.7120, 8.4151
Garg & Howe's	Tetragonal (I4/mcm): 6.066, 4.96	-0.169	6.073, 6.073, 4.855

S-phase (Al_2CuMg): There are also several models for the S phase based on experimental observations. The widely accepted structure is base-centered orthorhombic with space group $Cmcm$ and lattice constants $a=4.03$, $b=9.30$ and $c=7.08$. However, there is some dispute as to internal atomic coordinates. Our calculation, verifying a similar study[19], showed that the original model by Perlitz and Westgrin leads to a formation enthalpy of -0.210 eV/atom while exchange of the Cu and Mg in internal atomic coordinates, as suggested by Radmilovic *et al* [20], yielded a positive formation enthalpy of +0.289 eV/atom. By neglecting the entropy contribution (mostly from lattice vibration), this indicates that the Perlitz & Westgrin model is reasonable.

Interfacial Energy Between the 2nd Phases with Al Matrix: Interfacial energy of a second phase in the matrix is the key parameter for stability of precipitates and hence aid in determining the creep resistance of the alloys. Using the First Principle approach, the coherent interfacial energy between plate-like precipitates and the matrix can be calculated by setting up an appropriate super-cell containing the interfaces. The interfacial energy γ_i may be defined as

$$\gamma_i = \frac{E_{total} - n_\alpha E_\alpha - n_\beta E_\beta}{A_{(uv)}} \text{ where } E_\alpha \text{ and } E_\beta \text{ denote the formation energy of the precipitates and}$$

the matrix per atom, the n_α and n_β the number of the atoms contained in the supercell, and $A_{(uv)}$ is the area of the interface of the supercell. Figure 2 shows the supercell construction for calculation of the $\Omega(\theta_M)$ —Al (fcc) interfacial energy parallel to the Ω -habit plane $(111)_\alpha$ where the coinciding-site lattice in the interface was realized.

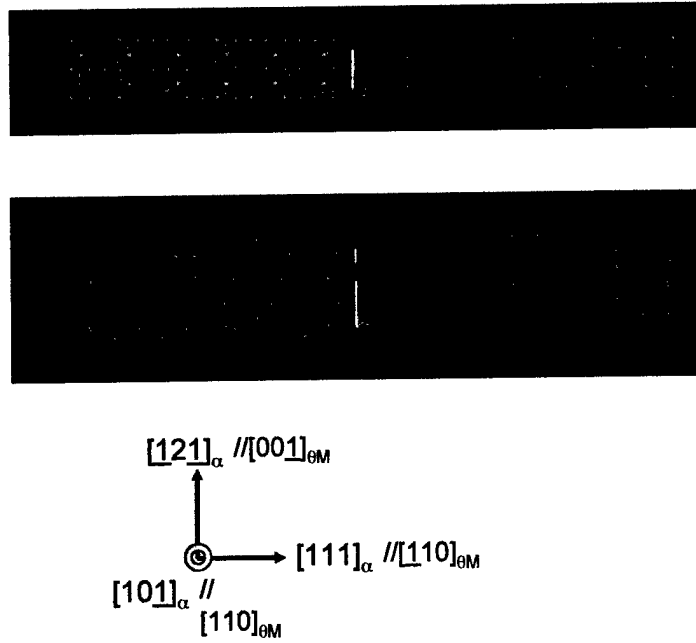


Figure 2. Supercell construction for calculation of the interfacial energy between Ω (θ_M) and Al (111). The top is the projection on YZ-plane and the middle is the projection on XZ-plane. The bottom shows the orientation match between the two phases. The pink balls represent Al-atoms and the brown Cu-atoms in the Ω -phase, and the blue are atoms in the Al-(fcc).

The ideal calculation is supposed to converge with the k-points meshing, energy cut-off and size of the supercell. A satisfactory result of 170 mJ/m², has been obtained for the θ' —Al(fcc) broad interface parallel with the habit plane {100}. The result of another independent calculation by V. Vaithyanathan *et al.* was 235 mJ/m² [21]. The calculations for other second phases are currently running on our computer. It is noted that since the internal atomic coordinates close to the interfaces are relaxed, the interfacial energy obtained consists of contributions from both chemical “bond- breaking” effect and the misfit strain energy. Again the results exclude the change in the entropy due to the interfaces. Interfacial energy calculations will also be used to select trace alloy additions that may reduce the interfacial energy and increase the thermal stability of the strengthening precipitates.

Deformation Behavior of Clusters and Precipitates: Quantitative data of the elastic constants for the 2nd phases are significant and fundamental for determining the strengthening mechanisms. These parameters also play a role in determining the habit-plane and the evolution of equilibrium shapes of the clusters and the 2nd phase particles since they determine the elastic strain energy associated with lattice misfit.

Direct measurement of the 2nd phase elastic constants of second phases is usually impractical. Quantitative analysis based on the elastic constants typically employ very rough estimates. First principle calculations can be employed to calculate the total energy of a crystal structure at 0 K. The 2nd order elastic constants of the crystalline solid at 0 K may be defined and calculated according to the variation in the energy from its optimized lattice structure as

$$C_{ijkl} = \left(\frac{\partial E}{\partial \varepsilon_{ij} \partial \varepsilon_{kl}} \right)_{E=E_{\min}} \text{ with } i, j, k, l = 1, 2, \text{ or } 3 \text{ where } E \text{ denotes the total energy, } \varepsilon_{ij} \text{ the strain}$$

tensor. Using “engineering” notations, Hooke’s law is applied: $\sigma_i = \sum_{j=1}^6 C_{ij} \varepsilon_j$ where σ_{ij} is the

stress tensor and S_{ij} the elastic compliance tensor. By applying strains in certain patterns, we can then retrieve the variation of the energy or the resulting stress tensor and calculate the elastic constants C_{ijkl} or S_{ijkl} . Table III lists the calculated results for Al, Cu, Ag, and Mg (hcp). We note that the results, although strictly for 0 K, are quite consistent with experimental measurements. The calculated results for θ' , θ , Ω and S-phase are listed in Table IV.

Table III. Elastic constants calculated using VASP and obtained from experiments at room temperature for some element crystals

Phase	Structure	Elastic Constants, 10^{10} N/m^2	
		Calculated	Experiments
Al	fcc	$C_{11}=9.30, C_{12}=6.38, C_{44}=3.13, B=7.35$	$C_{11}=10.8, C_{12}=6.13, C_{44}=2.85, B=7.2$
Cu	fcc	$C_{11}=17.9, C_{12}=12.4, C_{44}=8.03, B=14.27$	$C_{11}=16.84, C_{12}=12.14, C_{44}=7.54, B=13.7$
Ag	fcc	$C_{11}=10.93, C_{12}=8.39, C_{44}=3.73, B=9.24$	$C_{11}=12.4, C_{12}=9.34, C_{44}=4.61, B=10.36$
Mg	hcp	$C_{11}=5.39, C_{33}=4.78, C_{12}=2.39, C_{13}=3.26, C_{44}=1.75$	$C_{11}=5.64, C_{33}=5.81, C_{12}=2.32, C_{13}=1.81, C_{44}=1.68$

Table IV. Elastic constants calculated using VASP for some second phases

Phase	Structure	Elastic Constants, 10^{10} N/m^2
θ'	tetr.	$C_{11}=19.24, C_{33}=15.62, C_{12}=2.91, C_{13}=6.54, C_{44}=8.35, C_{66}=4.36$
$\Omega/\theta/\theta_m$	tetr.	$C_{11}=18.72, C_{12}=5.59, C_{13}=5.36, C_{33}=18.30, C_{44}=3.68, C_{66}=6.27$
S	orth.	$C_{11}=14.5, C_{22}=15.3, C_{33}=14.3, C_{12}=2.95, C_{13}=6.60, C_{44}=5.31, C_{55}=7.29, C_{66}=3.29$

Alloy Partitioning and the Al-Cu-Mg-(Ag) Phase Diagram: A series of isothermal diagrams for the Al-Cu-Mg ternary system are shown in Figure 3. It is important to note that the $(\alpha + \theta)/(\alpha + \theta + S)$ phase boundary shifts to higher Mg contents with increasing temperature, which is found at approximately 0.15 wt% and 0.50 wt% for 200°C and 300°C, respectively. This indicates a higher solid solubility for Mg, which limits the driving force for the formation of the S-phase, as temperature increases. A compromise must be reached concerning the Mg levels in the proposed alloys. In order to avoid S-phase precipitation the Mg contents must be kept to very low amounts (~ 0.10 wt%) and precisely controlled in these alloys. However, the allowable Mg content should be maximized in order to optimize the precipitation of Ω , recalling that it is necessary for nucleation at moderate temperatures. As a point of interest current experimental Al-Cu-Mg-Ag-X alloys lie within the $(\alpha + \theta + S)$ phase field for artificial aging at moderate temperatures (150-250°C) according to the calculated ternary isothermal sections. Also, it is important to note that this diagram does not account for the Ω phase. Rather, Ω precipitation is treated as a $\{111\}_{\alpha}$ variant of equilibrium θ , as previously mentioned.

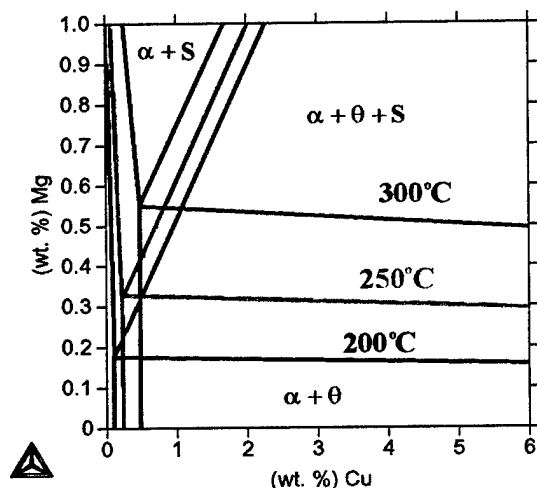


Figure 3. Calculated montage of isothermal sections of the Al-Cu-Mg ternary system.

We have verified Ringer *et al'* discovery [10] of Ag partitioning to the S-phase precipitates, as shown in Fig. 4. Systematic quantitative analysis of the Ag partitioning to S-phase precipitates is in progress. This analysis will provide the chemical composition of S-phase precipitates as a function of artificial aging temperature so that the energy descriptions for this phase in the Thermo-Calc database will account for the trace additions of Ag, rather than the stoichiometric ternary compound as modeled in the current database [15]. The quantitative information could also aid in the calculation of the interfacial energy between S-phase precipitates and the Al-rich matrix. Due to the complexity of the interface structure, first principle calculation of the interfacial energy is impractical.

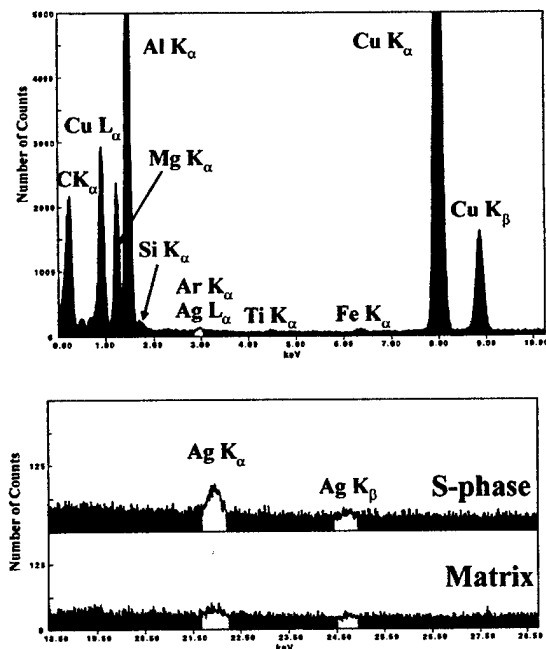


Figure 4. a) Representative EDS spectra collected from within a S-phase precipitate aged at 250°C for 1000h. b) High-energy regime of EDS spectra illustrating the partitioning of Ag to the S-phase precipitate relative to the surrounding matrix.

Effect of Silicon Content on Precipitation of the Ω Phase: Despite the rigorous studies performed on Al-Cu-Mg alloys from 1929-1954, the Ω phase, in the absence of Ag, was not identified until 1990. Revisiting a summary of the studies performed on Al-Cu-Mg alloys from 1929-1954 confirms that the Si content of the majority of the alloys studied exceeded 0.1^{wt}%. For many of these alloys, Si was intentionally added to increase strength (arising from enhanced matrix precipitation of the strengthening phases). These Si levels may have led to the suppression of Ω precipitation in these early Al-Cu-Mg alloys, and Ω was not observed until microstructural characterization was performed on high purity alloys.

Our experimental data [22] has demonstrated that Ω precipitation is suppressed in alloys with Mg/Si atomic fraction ratios of ≤ 2.0 , regardless of Si content and indicates that Ω precipitation is not dictated by a critical Si content, but rather by the Mg/Si ratio of the alloy. It is important to note that the critical Mg/Si ratio of 2.0 is consistent with the expected bonding between these two elements based upon atomic valency. Similarly, the Mg_2Si (β') precipitate formed in Al-Mg-Si alloys has an atomic Mg/Si ratio of 2.0.

Our results demonstrate that trace amounts of Si were responsible for limiting Ω precipitation in low Mg-containing alloys. They indicate that an atomic Mg/Si ratio of approximately 2.0 must be overcome for Ω nucleation. This sensitivity of Ω precipitation to Si content may explain the absence of Ω in early work on Al-Cu-Mg alloys and must be taken into consideration in our design of Al-Cu-Mg-(Ag) alloys for high strength and creep resistance at moderate temperatures.

Precursors and Non-Precursors for the 2nd Phases — SRO of Solutes: To achieve our objective to produce “fine, uniform precipitate-structures”, the strategy is to focus on boosting the nucleation rates of the favored strengthening precipitates through enhancement of the formation of their precursors by trace addition and/or elimination of harmful impurities.

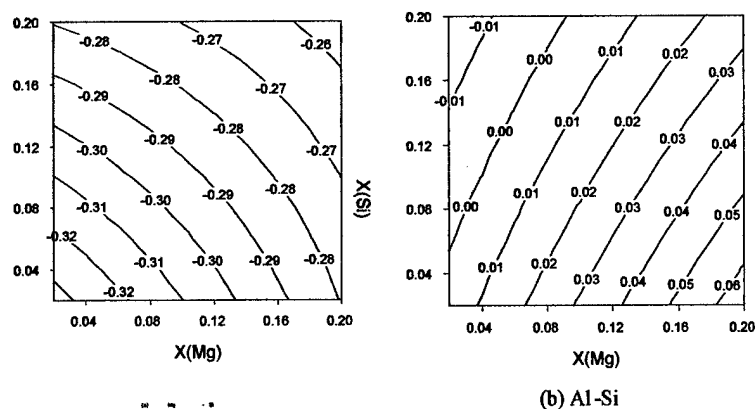


Figure 5. The short-range ordering parameters (a) $\alpha^{\text{Mg, Si}}$ of Mg-Si, and (b) $\alpha^{\text{Al, Si}}$ of Al-Si (Warren-Cowley parameter $\alpha^{A, B} = 1 - \zeta^{A, B} / x_A x_B$ where $\zeta^{A, B}$ denotes the pairing probability between A and B-

atoms) in Al-Mg-Si fcc-Al phase calculated using quasi-chemical approximation and CALPHAD databases – COST2.

The negative effect of Si in Al-Cu-Mg alloys mentioned above can be ascribed to the formation of short-range-ordering (SRO) like Mg-Si, that we call “non-precursors”, in the Al-FCC solid solution. It consumes the solutes needed for the precursors for the Ω -phase and hence jeopardizes its nucleation. We have set-up a method to evaluate SRO in order to rule out potential deleterious elements like Si in Al-Cu-Mg. The method is based on the quasi-chemical approximation with consideration of the 1st neighbor interaction [23]. The interaction parameters between each pair of elements are calculated using the heat of mixing of the alloy system under CALPHAD spirit. Using a sub-regular solution model as shown in Eq. (1) for a ternary FCC solution Al-Mg-Si, the heat of mixing may be written as

$$\Delta H_{mix} = \sum_{i,j} x_i x_j \sum_{v=0,m} (L^{(v)}_{i,j} - T \frac{\partial L^{(v)}_{i,j}}{\partial T})(x_i - x_{RM})^v + x_1 x_2 x_3 \sum_{k=0}^2 (L^{(k)}_{1,2,3} - T \frac{d L^{(k)}_{1,2,3}}{dT}) \quad (4)$$

where the interaction L-parameters can be retrieved from available Thermo-Calc databases. Fig. 5 shows the iso-values of the SRO parameters of Mg-Si and Al-Si in ternary system Al-Mg-Si – FCC solutions at 200°C. As indicated by very negative Warren-Cowley parameters when compared to the mostly positive values for Al-Si in the composition range interested, Si has a strong tendency to form Mg-Si SRO in the FCC (α) phase and hence to jeopardize the formation of Ω .

Conversely some trace element additions may have a very positive effect on nucleation of the desired $\{\Omega$ and $\theta'\}$ -phases as shown above. In the Al-Cu binary alloy, Cu tends to cluster on $\{100\}$ -planes in Al-Cu solutions. These clusters evolve into θ'' and θ' with $\{100\}_\alpha$ habit planes. However, the addition of Mg with Cu:Mg=10:1 leads to the tendency to form Ω plates on $\{111\}$. As indicated in the 3D-atomic probe (3D-AP) and HRTEM observation [9,10], this can be attributed to the clustering or short-range ordering (atom aggregates) as the precursors formed prior to the precipitation of the Ω phase. Analysis of elastic strain energy caused by these plate-like clusters may elucidate what Mg and/or Ag clusters may function as the precursors for Ω $\{111\}$ -phases. Assuming dilute solute approximation, we have set-up a method to calculate the

elastic strain energy dependence $E^{\{hkl\}_\alpha} = \frac{1}{2} C_{ijkl} \epsilon_{ij} \epsilon_{kl}$ on the orientation $\langle hkl \rangle_\alpha$ of the plate-like

clusters embedded in the Al-FCC matrix. The elastic constants C_{ijkl} were obtained using first-principle calculations. Fig. 6 shows the parametric plots of the orientation dependence of elastic strain energy for some clusters. It shows that the Cu-FCC ($C_{11}=17.90$, $C_{12}=12.46$, $C_{44}=8.03$) clusters has the highest strain energy as they are parallel with $\{111\}_\alpha$, and the lowest energy strain energy when parallel with $\{100\}_\alpha$. This explains the formation of Cu plate-like clusters on the planes $\{100\}_\alpha$, as experimentally observed Cu GP-zones in Al. The hypothesized Mg-FCC structure ($C_{11}=4.76$, $C_{12}=3.09$, $C_{44}=2.27$) is similar to Cu. Although the possible effect of interfacial energy on the shape of Mg clusters may explain why Mg-GP zones are spherical, the calculation indicates that pure Mg atoms are difficult to form plate clusters on $\{111\}_\alpha$ where they have the largest strain energy. Fig. 6 also shows a preliminary result for a “quasi-disordered” FCC-mixture of Cu and Mg (3:1). It shows that this mixture has the lowest strain energy when

parallel with $\{111\}_\alpha$. This indicates that it is the mixture clusters of Cu-Mg, that most likely form on $\{111\}_\alpha$, that functions as precursors for Ω precipitates. The strong calculated pairing probability or negative SRO-parameter for Mg-Cu supports this point.

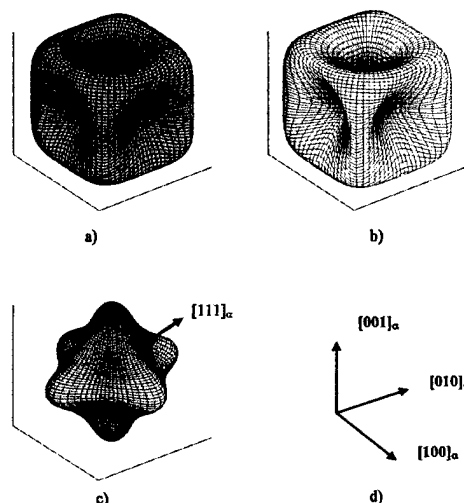


Figure 6. parametric plot of the orientation $\{hkl\}$ -dependence of elastic strain energy (under dilute approximation) caused by embedding a plate-like FCC cluster in Al-matrix oriented with respect to the Al-cubic coordinates. a) Cu-FCC; b) Mg-FCC (postulated); and c) a Cu₃Mg₁-FCC mixture. Insert d) indicates the cubic coordinates of the FCC-matrix.

We have established two factors to identify potentially “useful” trace elements for forming precursors and/or “harmful” impurities that form non-precursors: the SRO parameter that gauges probability for potential elements to form either SROs or clusters (atom aggregates), and the orientation-dependence of the strain energy that controls the habit-plane selection of these plate-like aggregates. Further SRO analysis depends on the more complete CALPHAD databases we are currently developing for Al-Cu-Mg-Ag-(X). The calculation of the elastic strain energy for the mixture or alloy clusters has employed the elastic constants obtained by First Principle calculations. Size limitation of the (“quasi-disordered”) supercell constructed due to computer capability does not allow for more realistic modeling of the disordered mixtures. Very recently, a robust technique was developed for calculation of elastic constants of disordered mixtures or alloys [24,25]. It is based on quasi-chemical approximation with consideration of atomic pair-interaction with the 1st and 2nd neighbors. The elastic constants are calculated from the axis-symmetric force constants of a virtual pair potential constructed for atoms interaction in the disordered alloys. The virtual potentials can be evaluated using curve-fitted data for pair bond-lengths from measured mean values or lattice parameters of the alloy crystals and/or from the known elastic constants of crystals (with the *same structure*) of the terminal pure elements. The technique can be applied to binary and ternary cubic alloys. It is noted that very often when terminal single crystals with the *same structure* are unavailable, the first principle calculation can be used for that input. Therefore, our future work will focus on combining the first principle calculations with this “virtual potential” technique for the orientation selection analysis of the embedded mixture-clusters *e.g.*, Ag-Cu, Ag-Mg, Mg-Ag-Cu, Zn-Cu etc, that are critical as potential precursors for the desired Ω and/or θ' -phases.

The Effect of Cold work on the Precipitation and Coarsening Behavior of Ω and θ' : The effect of plastic deformation on the microstructural evolution of an Al-5.0Cu-0.5Mg alloy was investigated in order to study how plastic deformation affects the competitive nucleation, growth and coarsening behavior of Ω and θ' in the absence of Ag [26]. Hardness measurements and quantitative precipitate analysis were performed on specimens that were water quenched from a solution heat treatment, stretched either 0% or 6% and immediately aged at ambient temperature or artificially aged at 200 °C or 250 °C for times up to 3000h. Quantitative transmission electron microscopy (TEM) was used to characterize Ω and θ' number density, diameter and thickness as a function of pre-age mechanical stretch and artificial aging condition. Age hardening curves for naturally and artificially aged specimens revealed an increase in hardness corresponding with a pre-age stretch. Quantitative TEM verified an increase in the number density and a refinement of precipitates for both Ω and θ' between the 0% and 6% stretch condition for those samples artificially aged. When aged at 200 °C, θ' exhibited superior coarsening resistance relative to the Ω phase. The quantified Ω coarsening kinetics was greater than similar Ag-containing alloys indicating that Ag may change the interfacial energy or the strain energy of the Ω precipitates.

References

1. W. Zhu, A. Csontos and E.A. Starke, Jr., *Acta mater.*, 1999, 47, 1713.
2. G. Liu, G. J. Zhang, J. Sun and K. H. Chen, *Mater. Sci. Eng. A*, 344, 1-2, 1-374 (2003)
3. I.J. Polmear and J.T. Vietz, *J. Inst. Met.*, 1966, 94, 410.
4. J.H. Auld, *Acta Cryst.*, 1972, A28, S98 Suppl.
5. S. Kerry and V.D. Scott, *Metals Sci.*, 1984, 18, 289..
6. K.M. Knowles and W.M. Stobbs, *Acta Cryst.*, 1988, B44, 207.
7. B.C. Muddle and I.J. Polmear, *Acta Metall.*, 1989, 37, 777.
8. A. Garg and J.M. Howe, *Acta Metall.*, 1991, 39, 1939.
9. L. Reich, M. Murayama and K. Hono, *Acta Mater.*, 1998, 46, 17, 6053.
10. S.P. Ringer, W. Yeung, B.C. Muddle and I.J. Polmear, *Acta Metall.*, 1994, 42, 5, 1715
11. C.R. Hutchinson, X. Fan, S.J. Pennycook and G.J. Shiflet, *Acta Metall.* 2001, 49, 2827
12. A.K. Mukhopadhyay, *Metall. Mater. Trans. A*, 1999, 30A, 1693.
13. EU COST507 project, Round II, 1998
14. ThermoTech Ltd., TT Al-based Alloys, 1999.
15. M.S. Lim, J.E. Tibballs and P.L. Rossiter, *Z. Metallkd.*, 1997, 88, 3, 237.
16. N. Unlu, B.M. Gable, G.J. Shiflet and E.A. Starke, Jr. *Mat. Sci. For.*, 2002;396-402:801.
17. B. M. Gable, M A Pana, GJ Shiflet, EA Starke Jr, *Mater. Sci. Forum* 396-402,699 (2002)
18. G. Kresse and J. Furthmueller, *J. Comput. Mater. Sci.*, 1996, 6, 15
19. C. Wolverton, *Acta mater.* 2001, 49, 3129.
20. V. Radmilovic, R.Kilaas, U Dahmen, G.J. Shiflet, *Acta mater.* 47, 3987 (1999)
21. V. Vaithyanathan, C .Wolverton, L. Q. Chen, private communication
22. B. M Gable, GJ Shiflet, EA Starke Jr, The effect of Si addition on the precipitation of Ω in Al-Cu-Mg-(Ag) alloys, *Scripta Mater.* 50, 2004, 149-153.
23. A W Zhu *et al.*, work in progress
24. Hartley C. S., *Acta Mater.* 51, 2003, 1373-1391.
25. Hartley C. S., private communication.
26. N. Unlu, B.M. Gable, G.J. Shiflet and E.A. Starke, Jr., The effect of cold work on the precipitation of Ω and θ' in a ternary Al-Cu-Mg alloy, *Met. Trans. A*. 34A, 2003, 2757-2769.

PERSONAL SUPPORTED

Brian M. Gable	Graduate Student, University of Virginia
Dr. Aiwu Zhu	Research Scientist, University of Virginia
Dr. Gary Shiflett	Reynolds Professor University of Virginia
Dr. Edgar A. Starke, Jr.	University and Ogelsby Professor, University of Virginia

PUBLICATIONS (Attached)

B.M. Gable, A.W. Zhu, G.J. Shiflet and E.A. Starke, Jr., "The Intelligent Design of Aluminum Alloys," in Materials Design Approaches and Experiences, Edited by J.C. Zhao, M. Fahrman and T.M. Pollock, TMS, 2001, pp. 111-122.

A.W. Zhu, B.M. Gable, G.J. Shiflet and E.A. Starke, Jr., (Invited Review) "The Intelligent Design of Age Hardenable Wrought Aluminum," Advanced Engineering Materials, Vol. 4, No. 11, 2002, pp. 839-846.

B.M. Gable, A.A. Csontos and E.A. Starke, Jr., "A Quench Sensitivity Study on the Novel Al-Li-Cu-X Alloy AF/C 458," Journal of Light Metals, Vol. 2, 2002, pp. 65-75.

A.W. Zhu, B.M. Gable, G.J. Shiflet and E.A. Starke, Jr., (Invited Plenary Lecture) "The Intelligent Design of High Strength, Creep-Resistant Aluminum Alloys," Materials Science Forum, Vol. 396-402, 2001, pp. 21-30.

B.M. Gable, M.A. Pana, G.J. Shiflet and E.A. Starke, Jr., "The Role of Trace Additions on the T₁ Coarsening Behavior in Al-Li-Cu-X Alloys," Materials Science Forum, Vol. 396-402, 2001, pp. 699-704.

N. Unlu, B.M. Gable, G.J. Shiflet and E.A. Starke, Jr., "The Effect of Cold Work on the Precipitation of Ω and Θ' in a Ternary Al-Cu-Mg Alloy," Materials Science Forum, Vol. 396-402, 2001, pp. 801-806.

B.M. Gable, G.J. Shiflet and E.A. Starke, Jr., "The Effect of Si Additions on the Nucleation of Ω in Al-Cu-Mg Alloys," TherMec 2003, Materials Science Forum, Vol. 426-432, 2003, pp. 471-476.

Aiwu Zhu, Brian M. Gable, Gary J. Shiflet, Edgar A. Starke, Jr., "Elastic Strain Energy Analysis of Trace-Element Clusters in Al-Cu-Mg-X Alloys: A First Principle Total Energy Calculation," in Proceedings of the 3rd International Conference on Light Materials for Transportation Systems, 2-6 November 2003, Honolulu, Hawaii.

N. Unlu, B.M. Gable, G.J. Shiflet and E.A. Starke, Jr., "The Effect of Cold Work on the Precipitation of Ω and Θ' in a Ternary Al-Cu-Mg Alloy," Metallurgical and Materials Transactions A, Vol. 34A, 2003, pp. 2757-2769.

B.M. Gable, G.J. Shiflet and E.A. Starke, Jr., "The Effect of Si Additions on Ω Precipitation in Al-Cu-Mg-(Ag) Alloys," Scripta Materialia, Vol. 50, 2004, pp. 149-153.

Edgar A. Starke, Jr. and James C. Williams, (Invited Plenary) "Light Alloys for Aerospace and Automotive Systems," in Proceedings of the 3rd International Conference on Light Materials for Transportation Systems," 2-6 November 2003, Honolulu, Hawaii.